Waste Management Bulletin 3 (2025) 100193

Contents lists available at ScienceDirect

Waste Management Bulletin

journal homepage: www.elsevier.com/locate/wmb

Optimizing drying of municipal dewatered sludge using heat-assisted microorganisms and pig manure addition: A process and economic analysis

Chencheng Wang [a], Zhigang He [a], Muhammad Usman [b], Mohamed Gamal El-Din [b,*], Zhigang Liu [a], Zhijun Luo [a], He Li [c], Dandan Xiao [c], Qunchao Qian [d], Zhiren Wu [a]

[a] School of the Environment and Safety Engineering, Jiangsu University, No. 301 Xuefu Road, Jingkou District, Zhenjiang 212013, PR China
[b] Department of Civil and Environmental Engineering, University of Alberta, Edmonton, Alberta T6G 1H9, Canada
[c] School of Civil Engineering, Southeast University, Nanjing 211189, PR China
[d] Jiangsu Key Laboratory for Environment Functional Materials, Suzhou University of Science and Technology, Suzhou 215009, PR China

ARTICLE INFO

Keywords:
Municipal dewatered sludge
Bio-drying
Multisource heat assistance
Pig manure
Hyperthermophilic bacteria
Evaluation

ABSTRACT

Sludge drying is an important pretreatment step for municipal dewatered sludge (MDS) treatment and disposal, but the time-consuming and high cost of existing processes have hindered the development of MDS treatment and disposal. In this study, a novel sludge drying technology was proposed on the basis of the characteristics and treatment needs of MDS in China. Pig manure (PM) addition and multisource heat assistance together assisted hyperthermophilic bacteria in achieving rapid drying of MDS. Mechanical factors were optimized via orthogonal experiments, and the optimum PM addition ratio was determined. The relationship between energy input (generation) and output in the system was explored to reveal the reasons why the novel drying technology exhibited superiority. Compared with the traditional biological drying technique and the thermal drying technique, the novel technique has the advantages of high efficiency, time savings and low cost. After 24 h of drying, the moisture content, organic matter content and net calorific value on an air-dried basis ($Q_{net,\,V,Mad}$) of the dried products were 31.43 ± 0.91 %, 72.47 ± 1.89 % and 16.94 ± 0.35 MJ/kg, respectively, which met the requirements of heat recovery and utilization for subsequent thermal treatment. The energy input (generation) to the system exceeded the energy output, indicating that the drying process was positively spontaneous. Multisource heat assistance accounted for 81.6 % of the total generated (input) energy, and 86.43 % of the energy was used for moisture evaporation, indicating high energy utilization of the drying system. In addition, cost savings of US $11.46–16.84/ton (¥83-122.10/ton) were achieved when MDS was treated via the novel drying technology. Overall, the novel drying technology proposed in this study provides feasible, efficient and cost-saving pretreatment technology and ideas for MDS treatment and disposal engineering.

Introduction

Municipal dewatered sludge (MDS) is a typical waste product produced by municipal domestic wastewater treatment plants (WWTPs) during the wastewater treatment process (Chang et al., 2023; Hao et al., 2020). In China, MDS is produced in large amounts, with more than 60 million tons/year on average in the last three years. As an organic solid waste, the treatment and disposal of sludge cannot be ignored (Chang et al., 2023; Usman et al., 2019). The main characteristics of sludge quality are high moisture content, low organic matter content, and high sand content (Qu et al., 2019). Pollutants in MDS include inorganics (e.g., flocculants, heavy metals, etc.) (Wei et al., 2018) and organics (PCBs, PAHs, disease-causing microorganisms, etc.) (Cao et al., 2021; Usman et al., 2023), whereas sludge is rich in organic matter, nutrients (nitrogen, phosphorus, potassium, etc.), and trace elements necessary for plant growth and development (calcium, magnesium, zinc, iron, etc.) (Hoang et al., 2022; Usman et al., 2020). Since MDSs exhibit both pollutant and resource properties, they need to follow the basic principles of reduction, harmlessness, stabilization, and resource utilization (Gao et al., 2022; Shi et al., 2021a). To meet China's market demand (Liang et al., 2023), various processes, such as aerobic fermentation & land use (Hoang et al., 2022), anaerobic digestion & land use (Shi et al.,

* Corresponding author at: 7-285 Donadeo Innovation Centre for Engineering, Department of Civil and Environmental Engineering, University of Alberta, Edmonton, Alberta T6G 1E9, Canada.
E-mail address: mgamalel-din@ualberta.ca (M.G. El-Din).

https://doi.org/10.1016/j.wmb.2025.100193

Available online 10 March 2025

2021b), incineration after drying & landfill of fly ash/manufacture of building materials (Liang et al., 2021), and deep dewatering & emergency landfill (Yang et al., 2015), have been developed after a long period of research and development.

Although a number of MDS treatments and disposal methods have been developed, all of them have been implemented on the basis of reducing the moisture content of the MDS to less than 40 % by drying pretreatment (Cai et al., 2016). Moreover, the dried products of MDS need to maintain a certain organic matter content and calorific value to facilitate subsequent treatment and disposal applications. Currently, commonly used sludge drying methods include natural drying, filtration pressure, thickening, thermal drying and bio-drying. Natural drying is a primitive method with shortcomings such as large floor space, severe secondary pollution and pest breeding (Liu et al., 2020). Filtration presses, including plate and frame presses (Cui et al., 2022) and belt presses (Olivier and Vaxelaire, 2005), are highly mechanically dependent (Li et al., 2020) and require large quantities of added chemical reagents (Tang et al., 2022) to perform the press, resulting in specialized treatment of the dried MDS. Thickening methods include centrifugation (Yan et al., 2018) and stacked-screw methods (Moustafa et al., 2022). After thickening, the sludge still has a high moisture content and needs to be further dried via other processes, which indirectly increases the treatment cost. Thermal drying is by far the most commonly used and efficient method and is one of the most energy intensive methods. Thermal drying can effectively kill pest eggs and promote moisture reduction (Wang et al., 2013). Generally, the heat used for sludge thermal drying comes from the conversion of electrical energy, which is a considerable cost. Although the utilization of waste heat as a source has been proposed, related research is still in the preliminary stage. Compared with other drying methods, research on bio-drying was developed later. The bio-drying method originates from aerobic composting technology, which is a method that utilizes the biological activities of microorganisms to promote moisture reduction in MDS (Wu et al., 2016). Bio-drying is an energy-saving process (Yu et al., 2023b), but it also has obvious shortcomings: first, the cycle time of bio-drying is long, usually 27–30 days, to achieve effective drying (Bilgin and Tulun, 2015); second, microorganisms decompose a large amount of organic matter in the MDS when drying is promoted, which has a negative impact on the subsequent utilization of the dried products (García et al., 1991). To compensate for the depletion of organic matter, it is necessary to add substances with high contents of organic matter, such as agricultural and forestry wastes, livestock wastes, and municipal kitchen wastes (Zhang et al., 2018), to the drying system. In addition to the above methods, researchers have developed electro-drying (Lv et al., 2018), microwave drying (Idris et al., 2004) and solar drying methods (Bux et al., 2002). However, these methods require considerable time and engineering validation from development to technological maturity, so thermal drying and bio-drying methods still have a high priority in various applications.

In this study, to address the need for rapid drying of MDS and overcome the shortcomings of existing drying technologies, a novel technology using PM addition and multisource heat assistance to assist hyperthermophilic bacteria in the rapid drying of MDS was proposed. This novel drying technology takes advantage of traditional thermal drying and bio-drying and solves the deficiencies of thermal drying and bio-drying through waste heat-based multisource heat reuse (simulated by heating wire) and PM addition, respectively. Specifically, given the shortcomings of energy consumption in traditional thermal drying, novel drying technology introduces multisource thermal assistance to solve this problem; the problem of excessive organic matter consumption exists in traditional bio-drying, which is effectively solved by the addition of PM in novel drying technology. In addition, due to the rapid increase in the mixture temperature during the drying process, which is detrimental to the survival of conventional microorganisms, high-temperature thermophilic bacteria were used in this study. Orthogonal experiments were used to optimize the mechanical factors (temperature, ventilation volume, and flip frequency) of the drying operation. The appropriate PM addition ratio was determined in terms of moisture content, organic matter content, $Q_{\text{net, V, Mad}}$ and material temperature before and after drying. The potential advantages of the novel drying technology were verified by comparing the differences in the drying effect and drying product properties between the novel drying technology proposed in this study and the traditional thermal drying technology and bio-drying technology. In addition, the reasons for the superiority of the novel drying technology proposed in this study were revealed in the context of the energy input (generation) and output relationship in the drying process, as well as the analysis of all the detailed cost savings involved during the drying process.

Materials and methods

Experimental materials

The MDS used in this study was obtained from a wastewater treatment plant (WWTP) in Jingkou District, Zhenjiang city, Jiangsu Province, China. This WWTP uses the University of Cape Town (UCT) process, which is an optimized Anaerobic-Anoxic-Oxic (A^2/O) process, to treat municipal wastewater. The excess activated granular sludge from the aerobic tank was flocculated by adding polyacrylamide (PAM) before entering the sludge thickener and then centrifuged and dewatered to obtain the MDS used in this study. The PM used in the mixture was taken from local farms and used in this study after being dried in natural sunlight. The MDS and PM samples were stored at 4 °C to eliminate the influence of nonexperimental factors such as microbial activity in the sludge and manure. The relevant parameters for the MDS and PM are detailed in Table S1.

The bacterial agent (BA) used in this study was JiuBang fermentation decomposer, which consists of thermophilic *Bacillus urealyticus*, *Bacillus megaterium*, *Bacillus subtilis*, *Lactococcus lactis*, and other high-temperature-resistant strains of bacterial species. During the MDS bio-drying process, *Bacillus urealyticus* exhibited high activity in a high-temperature environment and was able to decompose organic matter effectively. *Bacillus urealyticus* generates heat through metabolic activity, which contributes to moisture evaporation and organic matter decomposition in MDS. *Bacillus megaterium* has the advantage of breaking down complex organic matter and is able to secrete extracellular enzymes that help to break down bound moisture. *Bacillus subtilis*, which has a low activity threshold, helps decompose organic matter during MDS biodrying by producing enzymes and other metabolites and synergizes *Bacillus urealyticus* and *Bacillus megaterium* to improve drying efficiency. *Lactococcus lactis* could help to regulate the pH value of MDS by producing metabolites (lactic acid), thus indirectly promoting the growth and activity of other microorganisms. In summary, microorganisms interact with each other through synergistic effects to achieve rapid drying of the MDS. The detailed technical specifications of the BA are shown in Table S2.

Experimental equipment

A schematic diagram of the experimental setup is shown in Fig. 1. The core reactor was a drying chamber with an effective reaction volume of 40 L (the full reaction volume was 50 L). The material was added to the upper hatch of the chamber and allowed to react inside. The drying chamber was equipped with a stirring shaft, which enabled frequency-controlled stirring; a dehumidifier blower was attached to the side of the chamber for adjustable extraction. The drying chamber was connected to the deodorization chamber and the ammonia detector to reduce odor emission and monitor the discharge of gas in real time. In addition, heating wires were wrapped around the outer wall of the chamber to achieve the goal of heating the chamber to a specific temperature via a ramp-up control program. Part of the hot air discharged from the drying chamber can be reused for drying after

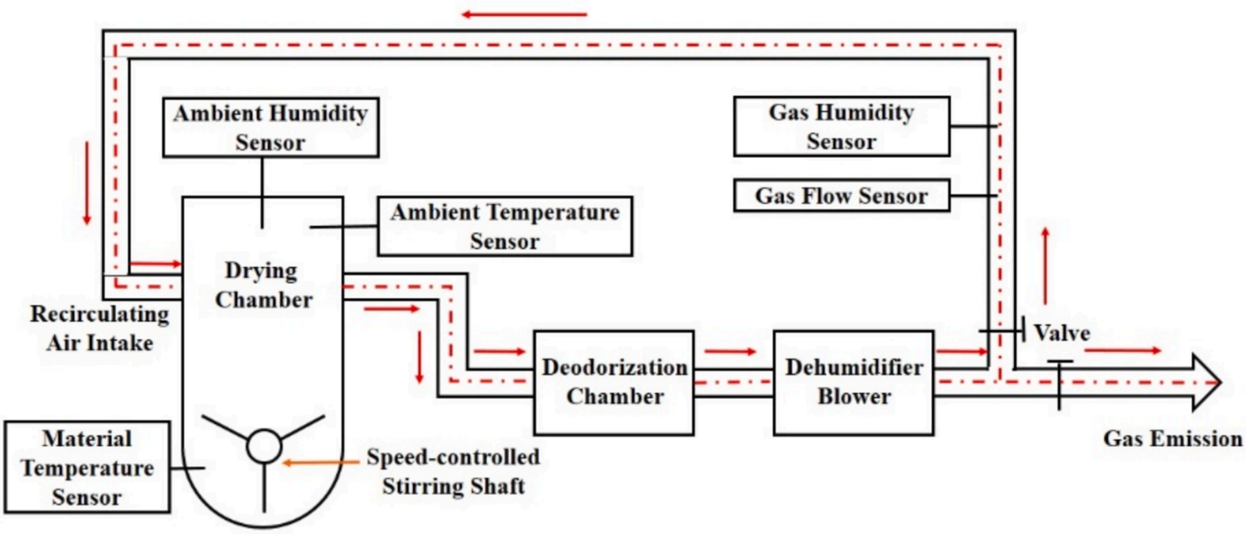

Fig. 1. Schematic diagram of experimental setup.

dehumidification, whereas the remaining hot air can be discharged directly after treatment. The whole device was equipped with several sensors, which can record the reaction temperature of the material and the temperature and humidity of the drying chamber in real time. The initial numerical control and the numerical value of the reaction process can be operated and viewed in the control panel.

Experimental design

Feasibility assessment tests

The sludge was subjected to different conditions to determine the effects of bacterial agents, the introduction of hot air, and the addition of auxiliary materials on the drying process of MDS. A total of five experimental groups were set up, namely, municipal dewatered sludge (Group (1), municipal dewatered sludge & bacterial agent (Group (2), municipal dewatered sludge & hot air (Group (3), municipal dewatered sludge & pig manure (Group (4), and municipal dewatered sludge & bacterial agent & hot air & pig manure (Group (5). In Group (1) (G1), 1 kg of untreated MDS was added directly to the drying chamber, and the experiments were conducted at room temperature. The experimental conditions for Group (2) (G2) were essentially the same as those for G1, except that the entire experiment was conducted at 55 °C. In Group (3) (G3), 1 kg of MDS and 10 g of BA were homogeneously mixed and added to the drying chamber, and the experiment was carried out at 55 °C. In Group (4) (G4), 0.8 kg of MDS and 0.2 kg of PM were mixed and added to the drying chamber, and the experiment was conducted at room temperature. In Group (5) (G5), 0.8 kg of MDS, 0.2 kg of PM and 10 g of BA were mixed and added to the drying chamber, and the experiment was conducted at 55 °C. In addition, the settings of the ventilation volume (5 s/min) and the turning frequency (continuous turning) were kept consistent for all five sets of experiments. The experimental groups were operated synchronously in the experimental setup, and the reactions were carried out continuously for 24 h. A total of 10 g of sample was collected at different times during the whole reaction process, and the moisture content was determined for comparison.

Orthogonal test for mechanical factors

Mechanical factors mainly refer to the difference in the drying effect of a material caused by changes in the operating conditions of the drying equipment. The mechanical factors in this study mainly include the temperature, ventilation volume, and flip frequency of the drying chamber. An orthogonal experiment is a design method for conducting and analyzing multivariate experiments via orthogonal tables, which includes selecting the most representative level combinations from the total combinations of the tested factors, analyzing the results of the tested subsets to obtain a picture of the whole test dataset, and finding the optimized level combinations (Wu et al., 2019). A three-factor, three-level orthogonal experiment was set up to analyze the combinations of temperature, ventilation volume and flip frequency. The orthogonal design was used for combination experiments, and samples were taken to determine the moisture content of the drying sludge after 24 h of continuous operation to analyze the optimal level combinations of the above three factors (Table 1).

To calculate the results, the K value, K value and R value were used together for mathematical analysis and optimization of the conditions. The K value is the sum of the indicators corresponding to the measured level data (Tan et al., 2023), and k is the average value of the indicators corresponding to the measured level data (Dong et al., 2023), reflecting the degree of influence on the detection of indicators at different levels.

Optimization experiment for the PM addition ratio

The external factors were set to the optimal level, and pig manure was selected as an auxiliary material to examine the drying behavior and effect of various mixing ratios on sludge drying. The total weight of the fixed mixture was 5 kg, and 50 g of bacterial agent (1 wt%) was added to each experimental group. In the present study, the MDS:PG ratios were set at 4:1 (Group (7), G7), 5:1 (Group (8), G8), 6:1 (Group (9), G9), and 7:1 (Group (10), G10). Moreover, an additional group of MDS:PM at a ratio of 1:0 was used as a control group (Group (6), G6). The samples from the five groups of experiments were reacted consecutively for 24 h, and the samples were taken at different stages of the reaction for the determination and analysis of different parameters.

Table 1
Orthogonal experiment $L_9(3^3)$.

Experiment	Temperature Level (°C)	Ventilation Volume Level (s/min)	Flip Frequency Level (times/h)
1	1 (50)	1 (3)	1 (1)
2	1 (50)	2 (4)	2 (0)
3	1 (50)	3 (5)	3 (n)
4	2 (55)	1 (3)	2 (0)
5	2 (55)	2 (4)	3 (n)
6	2 (55)	3 (5)	1 (1)
7	3 (60)	1 (3)	3 (n)
8	3 (60)	2 (4)	1 (1)
9	3 (60)	3 (5)	2 (0)

Comparison experiment

The advantages of the novel drying technology used in this study were explored by comparing the differences in drying effects and drying product properties among the drying technologies used in this study, conventional bio-drying technology and conventional thermal drying technology. In the novel drying experiment group (Group (11), G11), 0.8 kg of MDS, 0.2 kg and 10 g of BA were homogeneously mixed and added to the drying chamber, and the experiment was conducted at 55 °C. In the conventional bio-drying experimental group (Group (12), G12), 1 kg of MDS and 10 g of commercially available BA (main components: Brevibacillus laterospor, *Aspergillus fumigatus*, Actinomycetes and *Saccharomyces cerevisiae*) were homogeneously mixed and added to the drying chamber, and the experiment was conducted at room temperature. In the conventional thermal drying experimental group (Group (13), G13), 1 kg of MDS was added to the drying chamber, and the experiment was conducted at 70 °C. All groups used a ventilation volume of 5 s/min and a flip frequency of continuous turning. The experimental groups were operated synchronously in the experimental setup, and the reaction was carried out continuously for 24 h. The temperature of the material was monitored by temperature sensors every 2 h. The moisture content, organic matter content and $Q_{net,V,Mad}$. of the material were determined at 0 h and 24 h.

Characterization and calculation

Characterization

The drying index of the material was mainly examined in terms of moisture content, organic content (including volatile solids content) and net calorific value on an air-dried basis ($Q_{net,V,Mad}$). The determination methods for organic matter content and moisture content were carried out with reference to the weight method stipulated in part 1 and part 2 of CJ/T211-2005 (Determination method for municipal sludge in wastewater treatment plants), an industry standard for urban construction in the People's Republic of China. The net calorific value on an air-dried basis was determined via the method of ISO 1928:1995, Solid mineral fuel. The gross calorific value was determined via the bomb calorimetric method, and the net calorific value was calculated. The elemental analysis of the material was carried out via an organic elemental analyzer model Elementar: Vario UNICUBE.

Calculation

Bio-drying is a nonstationary intermittent process where the heat balance is maintained between the energy produced by the biological reaction and the energy consumed and lost throughout the process (Li et al., 2019). Heat balance calculations were performed to determine whether the heat generation in the system was sufficient to meet the heat consumption requirements. When calculating the heat balance of a drying process, it is usually necessary to make the following three assumptions: first, the system reaches a steady state, and the heat, organic matter and moisture are uniformly distributed in the mixture; second, the humidity gradient of the hot air is ignored, and the physical properties of the mixture are considered constant; and third, changes in environmental conditions are not taken into account. These simplified assumptions were helpful for the calculation but might be slightly different from the actual operation, which was factored into the margin of error. For the accuracy of the calculations, the heat generation included the heat produced by the organisms with multiple heat reuses, whereas the heat consumption included the heat utilized by evaporation of moisture and an increase in substrate temperature within the system, as well as the heat lost from conduction, radiation, and turning of the mixture (Li et al., 2018). The specific calculation formula is shown in Eq. (1) (Zhao et al., 2010):

$$\begin{aligned} Q_{bio}+Q_o &= Q_{consu}+Q_{loss} \\ &= Q_{dryair}+Q_{watvap}+Q_{water}+Q_{solid}+Q_{evapo}+Q_{radi}+Q_{condu}+Q_{turning} \end{aligned} \tag{1}$$

In Eq. (1), Q_{bio} represents the energy generated by the microbial reaction in the system; Q_0 represents the energy of multisource heat reuse;Q_{consu} represents the energy consumed in the drying process, including sensible heat and latent heat; and Q_{loss} represents the energy lost in the drying process, including radiant, conductive, and turnover loss energy. The sensible heat involved in the drying process is the heat consumed by aeration $Q_{dryair}+Q_{watvap}$ and the heat consumed by increasing the substrate temperature $Q_{water}+Q_{solid}$, while the latent heat is the heat consumed by moisture evaporation Q_{evapo}; the heat lost from thermal radiation, heat conduction and stacking are Q_{radi}, Q_{condu} and $Q_{turning}$, respectively. The above parameters were expressed in kJ.

The detailed formulas for each parameter are shown in Eq. (2) to Eq. (13) below:

$$Q_{bio} = BVS \times H_c \tag{2}$$

In Eq. (2), (Zhao et al., 2010), BVS (g) represents the amount of change in VS during the reaction; H_c represents the empirical calorific value of the biodegradable organic matter, which was 23.2 kJ/g.

$$Q_{dryair} = M_{air} \times C_{dryair} \times (T_m\text{-}T_a) \tag{3}$$

$$Q_{watvap} = M_{air} \times \omega \times C_{watvap} \times (T_m\text{-}T_a) \tag{4}$$

In Eq. (3) and Eq. (4), (Hao et al., 2018), M_{air} is the weight of dry air (kg), which is related to the size and duration of daily ventilation; C_{dryair} is the specific heat of dry air, with a value of 1.004 kJ/(kg·°C); C_{watvap} is the specific heat of moisture vapor, with a value of 1.841 kJ/(kg·°C); ω is the humidity of the incoming air after passing through the material layer (%); and T_m (°C) and T_a (°C) are the material temperature and ambient temperature, respectively.

ω was obtained via the joint calculation of Eq. (5) and Eq. (6) (Huilinir and Villegas, 2015; Zhou et al., 2021):

$$\omega = \frac{MW_{H_2O}}{MW_{air}} \times \frac{P_{vs} \times RH}{P\text{-}(P_{vs} \times RH)} \tag{5}$$

$$P_{vs} = 10^{\left[\left(\frac{a}{T_m+c}\right)+b\right]} \tag{6}$$

In Eq. (5) and Eq. (6), MW_{H_2O} and MW_{air} are the molar masses of moisture and air, taken as 18 g/mol and 29 g/mol, respectively; P_{vs} and P are the saturated vapor pressure (Pa) and inlet air pressure (Pa), respectively; RH is the relative humidity in %; and a, b, and c are dimensionless constants, taken as the values −2238, 8.896, and 273, respectively.

$$Q_{water} = M_{water} \times C_{water} \times \Delta T_m \tag{7}$$

$$Q_{solid} = M_{solid} \times C_{solid} \times \Delta T_m \tag{8}$$

In Eq. (7) and Eq. (8), (Cheng et al., 2021), M_{water} (kg) and M_{solid} (kg) are the weights of moisture and dry solids in the material, respectively; C_{water} and C_{solid} are the specific heat capacities of moisture and dry solids at 4.184 kJ/(kg·°C) and 1.046 kJ/(kg·°C), respectively; and ΔT_m (°C) is the change in temperature of the material over a period of time.

$$Q_{evapo} = M_{eva} \times L_{latwat} \tag{9}$$

$$L_{latwat} = (1093.7\text{-}0.5683 \times \frac{T_m+32}{5} \times 9) \times \frac{1055}{454} \tag{10}$$

In Eq. (9) and Eq. (10) (Mason, 2009), M_{eva} (kg) is the weight of evaporated moisture, and L_{latwat} (kJ/kg) is the evaporated latent heat of moisture, which is calculated from Eq. (10).

$$Q_{radi} = A_{top} \times \sigma \times F_a \times F_e \times (T_t^4\text{-}T_a^4) \quad (11)$$

where (Ahn et al., 2007), A_{top} (m^2) is the surface area of the material; σ is the Stefan–Boltzmann constant, which is 5.67×10^{-11} kJ/(s·m^2·K^4); T_t (°C) is the temperature of the top layer of the material; and F_a and F_e are dimensionless coefficients of 0.50 and 0.85, respectively.

$$Q_{condu} = U \times A \times (T_m\text{-}T_a) \quad (12)$$

In Eq. (12), (Yu et al., 2022), U is the heat transfer coefficient of the reactor wall, which is 0.5×10^{-4} kJ/(d·m^2·°C), and A (m^2) is the reactor wall area.

$$Q_{turning} = M_{water} \times C_{water} \times (T_m\text{-}T_a) + M_{solid} \times C_{solid} \times (T_m\text{-}T_a) \quad (13)$$

Results and discussion

Feasibility testing analysis

The moisture content changes in the different experimental groups are shown in Fig. 2. Before and after drying, the moisture content of G1 decreased from only 85.72 ± 1.56 % to 84.48 ± 1.51 %, indicating that the promotion effect of natural drying on moisture reduction in the short term was negligible. Related studies have shown that although MDS is rich in microorganisms, the main function of the original microorganisms was for municipal wastewater treatment and not for bioheat production (Yu et al., 2023a). Despite the introduction of hot air, the moisture content of G2 decreased from 85.61 ± 1.56 % to 77.64 ± 1.21 %. The contribution of heat to moisture reduction in MDS was limited because of the intolerance of primary microorganisms in MDS to high temperatures. After the simultaneous introduction of hyperthermophilic bacteria and hot air (G3), a significant reduction in moisture content from 85.61 ± 1.56 % to 80.56 ± 1.34 % was achieved within 18 h. The insignificant change in moisture content after 18 h was attributed to the limited organic matter content in the MDS. Hyperthermophilic bacteria produce large amounts of bioheat when organic macromolecules are decomposed into micro molecules, which is beneficial for reducing the moisture content of MDS. Moreover, organic matter provides the material and energy needed for the metabolism and reproduction of hyperthermophilic bacteria. In G3, the organic matter in the MDS was not replenished after it was consumed, which produced negative feedback on microbial life activities. After PM was added to the MDS (G4), the moisture content was immediately reduced to 74.09 ± 1.56 %, which was caused by the initial moisture content of the PM being lower than that of the MDS. Moreover, the data variation in G4 revealed that single organic matter supplementation did not have a direct effect on continuous moisture content reduction. The moisture reduction in G5 was a sustained and obvious process, which decreased from 73.92 ± 1.34 % to 53.28 ± 0.98 %. The results of the five sets of experiments collectively demonstrated that a synergistic effect of thermal, microbial and organic matter supplementation was required to achieve effective moisture reduction in MDS in a short period of time.

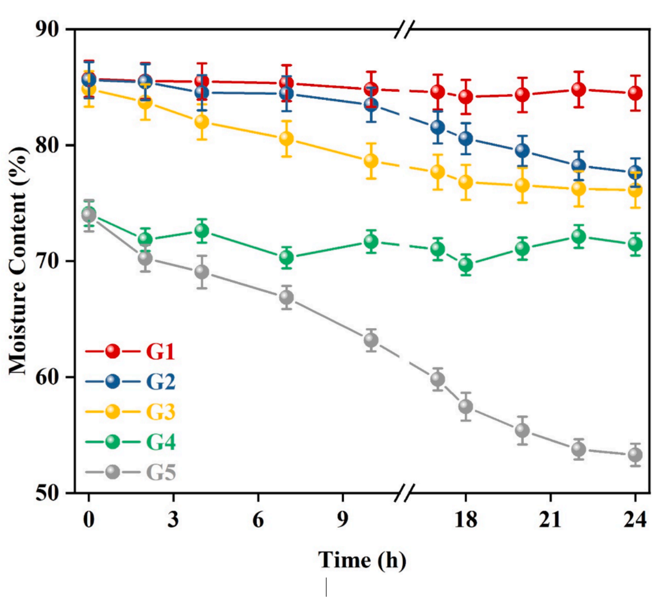

Fig. 2. Moisture content changes of different experimental groups within 24 h.

Mechanical factor analysis

The combined experiments were conducted via an orthogonal design (Table 2), which was continuously run for 24 h. The temperature, ventilation volume, and flip frequency significantly influence sludge drying and have a mutual coupling relationship. The sludge moisture content was used as the evaluation index, and the experiment was carried out according to the L9 orthogonal table 33 (Table 3). A lower moisture content represented more effective MDS drying, so the conditions corresponding to the lowest k values were considered the optimal choice for the analysis of the orthogonal experimental data. The lowest k values corresponding to temperature, vaporization volume and flip frequency were 68.68 ± 1.94 (k2), 68.62 ± 2.11 (k3) and 64.22 ± 1.45 (k3), respectively. When the temperature was set to 50 °C, the activity of the added hyperthermophilic bacteria was not fully activated, and the decrease was insignificant, although it showed some moisture reduction effect; when the temperature was increased to 55 °C, the hyperthermophilic bacteria were completely activated and produced a large amount of bioheat (Li et al., 2018), so the moisture content decreased substantially; when the temperature was further increased (60 °C), the hyperthermophilic bacteria activity was partially inhibited, which resulted in a lower moisture reduction performance than that at 55 °C. The moisture content decreased with increasing ventilation volume because most hyperthermophilic bacteria used in this study were aerobic or partially anaerobic (Mohammed et al., 2017). Therefore, a high ventilation volume meant that the hyperthermophilic bacteria in the mixture had sufficient contact with hot air containing more oxygen. The large amount of heat produced by the hyperthermophilic bacteria promoted the evaporation of moisture from the MDS. In addition, the fast-flowing hot air also carried the evaporated moisture out of the drying system, further pushing the moisture content in a lower direction. For the flip frequency, k2 was much greater than k1 and k3. Stationary bacteria on the surface of the mixture perform aerobic activities, and the bacteria inside the mixture are blocked from contact with the hot air and thus perform anaerobic activities. This nonuniform biological behavior produced an inhomogeneous distribution and evaporation of moisture, which in turn weakened the moisture reduction effect. When continuous flipping was performed, all hyperthermophilic bacteria carried out aerobic activities. Moreover, the flipping facilitated the evaporation of the moisture in the mixture into the air flow, which ultimately demonstrated excellent moisture reduction. An analysis of variance (ANOVA) was performed on the orthogonal experimental metrics, and the results are shown in Table 4. The temperature, ventilation volume and flip frequency significantly affected the experimental results. Specifically, the F values of these three factors were 23.96, 37.18 and 247.63, respectively, which were much higher than the corresponding critical F values (calculated to be 19). The corresponding p values were 0.040,

Table 2
Factor level for orthogonal experiment $L_9(3^3)$.

Level	Temperature (°C)	Ventilation Volume (s/min)	Flip Frequency (times/h)
1	50	3	1
2	55	4	0
3	60	5	n

Table 3
Results and polar differences for orthogonal experiment $L_9(3^3)$.

Serial Number	Temperature (°C)	Ventilation Volume (s/min)	Flip Frequency (times/h)	Moisture Content (%)	95 % Confidence Interval
1	1 (50)	1 (3)	1 (1)	74.11 ± 2.87	[71.90, 76.32]
2	1 (50)	2 (4)	2 (0)	79.32 ± 1.94	[77.83, 80.81]
3	1 (50)	3 (5)	3 (n)	64.74 ± 1.53	[63.56, 65.92]
4	2 (55)	1 (3)	2 (0)	79.02 ± 2.04	[77.45, 80.59]
5	2 (55)	2 (4)	3 (n)	60.94 ± 1.32	[59.93, 61.95]
6	2 (55)	3 (5)	1 (1)	66.07 ± 2.47	[64.17, 67.97]
7	3 (60)	1 (3)	3 (n)	66.98 ± 1.49	[65.83, 68.13]
8	3 (60)	2 (4)	1 (1)	66.31 ± 1.75	[64.96, 67.66]
9	3 (60)	3 (5)	2 (0)	75.06 ± 2.33	[73.27, 76.85]
K1	218.17 ± 6.34	220.11 ± 6.40	206.49 ± 5.01		
K2	206.03 ± 5.83	206.57 ± 5.01	233.40 ± 6.31		
K3	208.35 ± 5.57	205.87 ± 6.33	192.66 ± 4.34		
k1	72.72 ± 2.11	73.37 ± 2.13	68.83 ± 1.67		
k2	68.68 ± 1.94	68.86 ± 1.67	77.80 ± 2.10		
k3	69.45 ± 1.86	68.62 ± 2.11	64.22 ± 1.45		

Table 4
ANOVA for orthogonal experiment $L_9(3^3)$.

Variance Source	Sum of Squares of Deviations	Degrees of Freedom	Mean Square	F-Value	p-Value
Temperature (°C)	27.688	2	13.844	23.963	0.040
Ventilation Volume (s/min)	42.955	2	21.478	37.176	0.026
Flip Frequency (times/h)	286.129	2	143.065	247.631	0.004
Error	1.155	2	0.578	–	–

0.026 and 0.004, which were all less than 0.05 (Renqingcairang et al., 2022), indicating that the data were significantly different. Among these three factors, the flip frequency had the most significant effect, with the highest F value, indicating that it was the most critical factor affecting moisture reduction. Moreover, the low value of experimental error reflected the good repeatability of the experiment and the high reliability of the data. On the basis of the above analysis, the optimized combination of equipment parameters was set as follows: the temperature was 55 °C, the ventilation volume was 5 s/min, and the flip frequency was continuous turning.

Optimization analysis

The above optimized mechanical factors were applied to explore the effects of different ratios of MDS and PG on drying and indexes.

Morphology analysis

Fig. 3 shows the morphology of the dried mixtures with different MDS:PM ratios after 24 h of reaction. All the materials presented a brownish yellow color and did not emit odors, indicating that the mixture was in an aerobic composting state. When the content of oxygen and organic matter in the system was high and the temperature reached a certain level, the hyperthermophilic bacteria could fully metabolize and produce bioheat, which was favorable for moisture reduction. The morphology of the reactants significantly varied across different ratios. With an increase in the percentage of pig manure, the material structure became more porous, resulting in a decrease in moisture content within the reacted material. For G9 and G10, the dried material exhibited a solid bulk structure with viscosity and retained a noticeable moisture content. In G8, the structure began to loosen, whereas in G7, the final product manifested as loose small particles with a significant reduction in moisture content. The variability in the macroscopic morphology of the materials suggested the direct influence of ratios on moisture content, highlighting the need for subsequent parametric analysis.

Basic characteristics analysis

As shown in Fig. 4a, the initial moisture contents of G7-G10 were lower than those of G6, and within the experimental group, the moisture content decreased with increasing PM proportion, which was attributed to the lower initial moisture content of PM than that of MDS. The moisture content of G6 after drying was reduced to 52.81 ± 1.32 %, directly indicating that optimized mechanical conditions were beneficial for moisture reduction in the mixture. The sequence of initial moisture content was similar after 24 h of drying; however, the differences in moisture content among the various experimental groups became more pronounced after drying. Furthermore, the moisture reduction rates of the experimental group were 57.51 % (G7), 49.73 % (G8), 45.73 % (G9) and 39.27 % (G10), which were higher than those of G6 (37.62 %). The aforementioned phenomena collectively confirmed that the excellent drying effect was achieved through the combination of a low initial moisture content and high PM proportion (Teng et al., 2023). Related studies have shown that effective drying can be achieved when the moisture content of MDS is less than 40 % from the perspective of moisture content (Lin et al., 2023). On the basis of this moisture content threshold (40 %), there was a boundary between G8 and G9, i.e., the MDS was effectively dried when the addition of PM exceeded 16.67 wt %.

The variation in the organic matter content in the experimental and control groups before and after drying is shown in Fig. 4b. The organic matter consumption rate of G6 reached 16.55 %, indicating that hyperthermophilic bacteria significantly consumed organic matter in MDS during the drying process (Luo et al., 2020). In contrast to the moisture content, the initial organic matter content of G7-G10 was greater than that of G6, which was attributed to the high amount of organic matter introduced by the PM to the mixture. Moreover, the organic matter content of the experimental group remained high after drying, which was attributed to the fact that the introduction of PM fulfilled the demand of organic matter consumption by hyperthermophilic bacteria and compensated for the high consumption of organic matter by bacteria (Li et al., 2022). PM replenished the organic matter consumed in the mixture, which was crucial for the dried mixture during subsequent thermal treatment. Among the four experimental groups, although G7 had the highest organic matter consumption rate (3.21 %), its organic matter content was still higher than that of the other experimental groups, which was attributed to the high percentage of PM in the mixture. Previous studies have suggested that reducing the moisture content while increasing the organic matter content of a mixture can satisfy the minimum value of self-sustaining incineration and heat recovery and utilization, which is beneficial for reducing energy consumption during the disposal process (Ruiz-Gómez et al., 2017). For

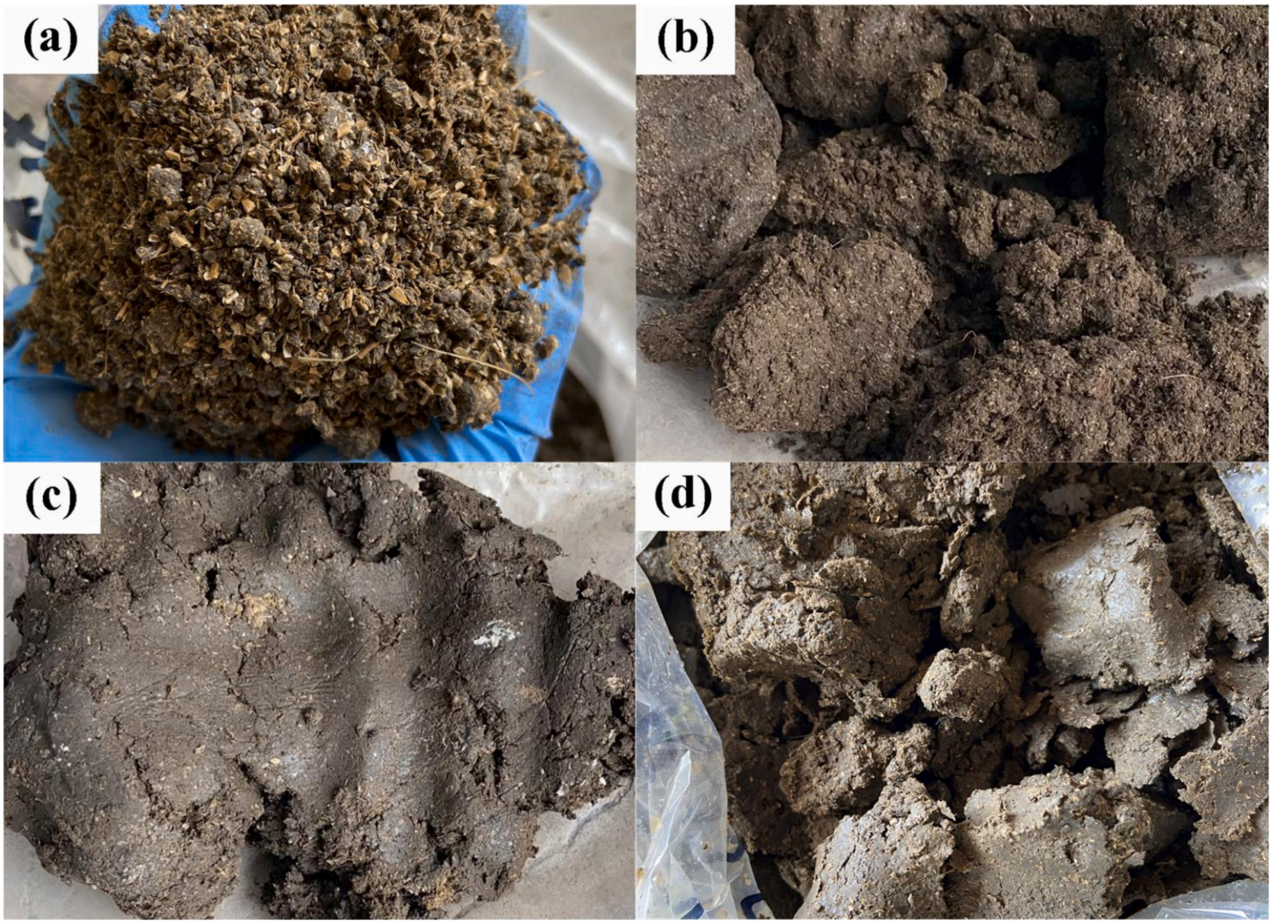

Fig. 3. Morphology images of the experimental groups with different ratios of dewatered sludge: pig manure after 24 h of drying: (a) 4:1, (b) 5:1, (c) 6:1, and (d) 7:1.

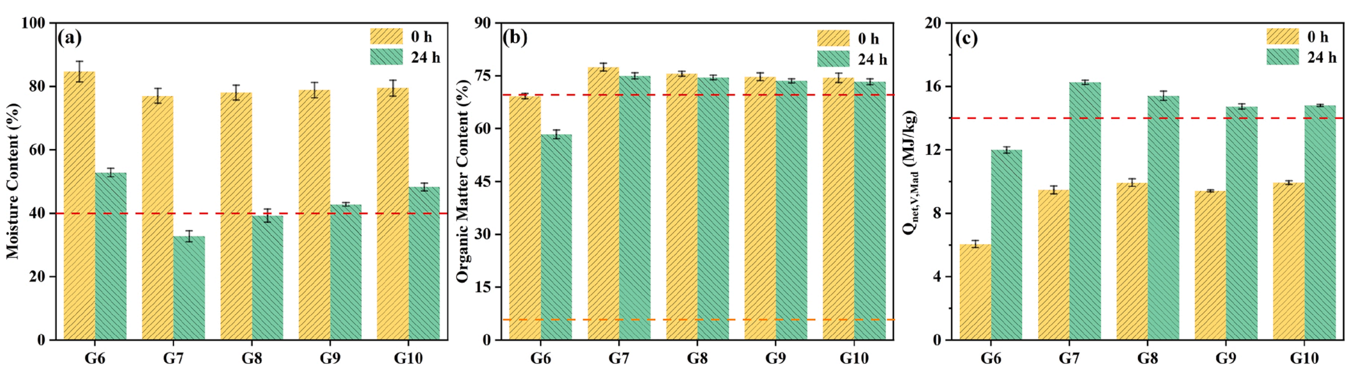

Fig. 4. (a) moisture content, (b) organic matter content, (c) $Q_{net,V,Mad}$ of materials in each group at 0 h and 24 h.

example, when agricultural biomass was added, sludge with a moisture content reduced to 58.67 % could undergo self-sustaining incineration; when the biomass addition proportion was increased, the moisture content of the mixture was further reduced to 49.48 %, which allowed for effective heat recovery and utilization (Li et al., 2023). Therefore, in this study, it was necessary to appropriately increase the PM proportion in the mixture while meeting the minimum requirement of the MDS drying effect.

The $Q_{net,\ V,\ and\ Mad}$ values of the different groups before and after drying are displayed in Fig. 4c. In comparison, the $Q_{net,\ V,\ and\ Mad}$ values of the PM-containing G7-G10 mixtures were greater than those of the G6 mixtures before and after drying, indicating that the addition of PM not only reduced the moisture content and organic matter compensation but also increased the $Q_{net,\ V,\ and\ Mad}$ values of the mixtures. Hyperthermophilic bacteria decompose organic macromolecules into organic micro molecules, increasing the potential calorific value of the stabilized chemical bonds of macromolecules. For the initial $Q_{net,V,Mad}$, although the calorific value of each group met the lower calorific value requirement (5.00 MJ/kg) for self-sustaining sludge incineration, as stipulated in the national standard of the People's Republic of China GB/T 24602–2009 (Disposal of sludge from municipal wastewater treatment plant-Quality of sludge used in separate incineration) (Jin et al., 2014; Wei et al., 2020; Yang et al., 2015; Zhang et al., 2021), the corresponding initial moisture content exceeded 50 %, which was the main hindrance for subsequent thermal treatment. After drying, the organic matter content in G7-G10 slightly decreased, whereas $Q_{net,\ V,\ and\ Mad}$

increased significantly, with $Q_{net, V, and Mad}$ increasing rates of 71.59 % (G7), 55.19 % (G8), 56.81 % (G9) and 49.14 % (G10), respectively. This slight decrease in organic matter content was attributed to the respiratory and metabolic reactions of hyperthermophilic bacteria in an activated state, whereas the noticeable increase in caloric value was caused mainly by the decrease in moisture content. Moreover, the added PM brought more combustible organic matter into the mixture, which directly improved the caloric value.

Researchers discovered that when dried sludge was subjected to subsequent thermal treatment and heat recovery and utilization, the moisture content, organic matter content, and $Q_{net, V,}$ and Mad were less than 40 %, greater than 70 %, and greater than 14 MJ/kg, respectively (Liu et al., 2023). Combined with Fig. 4a-c, only G7 and G8 fulfilled the relevant requirements. In this study, the introduction of PM into MDS not only improved drying performance but also reflected the environmental protection concept of "waste for waste". Therefore, in drying applications, increasing the PM proportion in the mixture was given priority.

Process temperature analysis

The temperature changes in the mixture and drying chambers of the control group and experimental groups are presented in Fig. 5. The drying chamber temperature was maintained at a stable 55 °C, confirming the good stability of the drying unit. Since the heating of the drying chamber simulates multisource heat reuse in a scaled process, the continuous and stable thermal effect could effectively shield the equipment from errors and facilitate heat balance calculations. A comparison of the temperature changes throughout the drying process revealed that the temperature of the mixture material in the experimental groups (G7-G10) was always greater than that of the control group (G6), indicating that the hyperthermophilic bacteria were able to consistently utilize the organic matter in the mixture material to produce bioheat after the addition of PM. Bio-heating not only promoted moisture evaporation but also increased the temperature of the mixture, which in turn contributed to the maintenance of hyperthermophilic bacterial activity. In addition, the material temperature increased with increasing PM proportion because organic matter compensation promoted the biological activity of hyperthermophilic bacteria and indirectly increased bioheat production (Zhao et al., 2010). The material temperature of G7 was essentially maintained above 50 °C, implying that the hyperthermophilic bacteria in G7 were always active throughout the drying process. For the experimental group, during 0–3 h of the drying process, hyperthermophilic bacteria were activated and rapidly proliferated with the assistance of multisource heat reuse (simulated by a heating wire). A slight decrease in the material temperature was subsequently observed at 3–17 h. The reason for the above phenomena was that there was a limit on the amount of PM added, and the compensated organic matter could not fully satisfy the demand of all hyperthermophilic bacteria, which led to a decrease in the number of hyperthermophilic bacteria as well as the output of bioheat, which manifested as a decrease in the material temperature. After 17 h, the number of hyperthermophilic bacteria decreased to the point where organic matter could continue to fully satisfy microbial biological activities, and the output of bioheat was restored, leading to a rebound in the material temperature. For G6, due to the absence of organic matter supplementation, the organic matter consumed by hyperthermophilic bacteria was supplied only by MDS, so the material temperature continued to decrease after drying was carried out for 4 h.

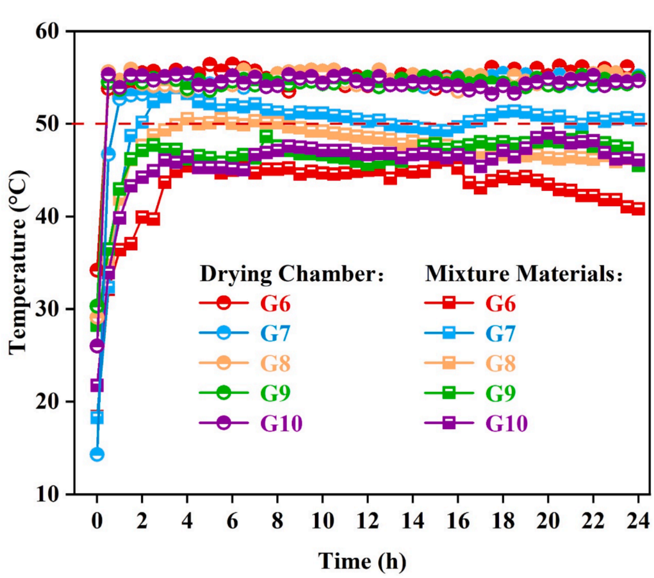

Fig. 5. Temperature changes of mixed materials and drying chamber within 24 h of drying.

From the point of view of moisture content, organic matter content and $Q_{net,V,Mad}$, the conditions of G7 and G8 were consistent with the limitations of the subsequent thermal treatment. During the drying process, the material temperature of G7 was essentially maintained above 50 °C at all times, and the role of hyperthermophilic bacteria was utilized to the greatest extent possible. Therefore, after comprehensive consideration, the PM addition parameter used for G7, i.e., MDS:PM = 4:1, was selected as the standard addition ratio for subsequent studies.

Comparison with conventional bio-drying and conventional thermal drying methods

Fig. 6a shows the temperature changes in G11-G13 during the drying process. Consistent with the trend in Fig. 5, the temperature in G11 increased within 3 h and remained stable above 50 °C in the subsequent drying stage. In G12, due to the lack of thermal assistance, the temperature rose slowly over a 24-h period. In subsequent experiments, although the microorganisms in G12 were able to similarly increase the temperature above 50 °C, the process took approximately 7–10 d, which was much more time-consuming than that in G11. Moreover, the complete bio-drying stage took approximately 27 d, indicating that the time cost of conventional bio-drying far exceeded that of the novel drying technology used in this study. In G13, the temperature continuously increased from 0 h to 14 h and surpassed that in G11 at approximately 11 h. However, thermal drying usually requires a large amount of electricity, which indirectly increases the operating cost of the drying process.

Fig. 6b-d shows the moisture content, organic matter content and $Q_{net,V,Mad}$ values of G11-G13 before and after drying, respectively. The moisture contents of G11-G13 after drying were 31.43 ± 0.91 %, 78.35 ± 1.08 % and 51.63 ± 1.88 %, respectively, whereas the corresponding organic matter contents were 72.47 ± 1.89 %, 62.42 ± 1.28 % and 65.98 ± 0.83 %, respectively. The moisture content and organic matter content of G11 met the limits required in the standard, which was attributed to the synergistic effect of multisource thermal assistance, hyperthermophilic bacteria and PM addition. The drying process of G12 was long and delayed, and BA caused some depletion of organic matter in MDS, so the dried products presented high moisture contents and low organic matter contents. Despite the excellent temperature performance of G13, the moisture content was not effectively reduced because thermal action favored only free and adsorbed moisture in MDS, whereas bound moisture was difficult to remove. The removal of bound moisture requires higher drying temperatures or the action of microorganisms, which is a significant drawback of conventional thermal drying. Since the dried products need to be applied for subsequent thermal treatment, $Q_{net, V, and Mad}$ have become important indicators of product performance. In comparison, the $Q_{net, V, and Mad}$ of G11 (16.94 ± 0.35 MJ/kg) were greater than those of G12 (10.03 ± 0.27 MJ/kg) and G13 (10.72 ± 0.24 MJ/kg), and only G11 fulfilled the requirements of heat recovery

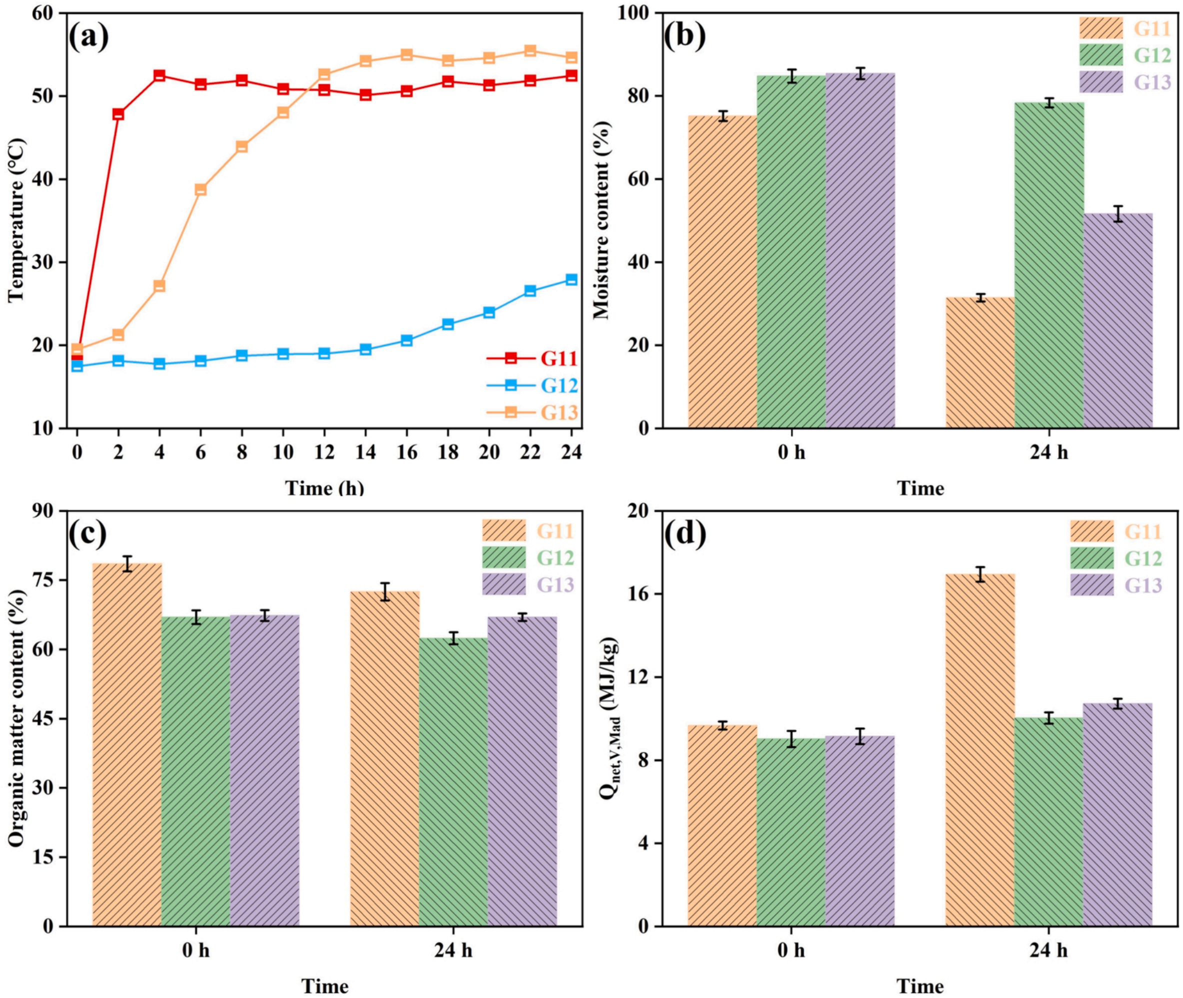

Fig. 6. (a) Temperature, (b) Moisture content, (c) Organic matter content and (d) $Q_{net,V,Mad}$ of dried materials in novel drying technology, the conventional bio-drying technology and the conventional thermal drying technology.

and utilization, indicating that the addition of PM played a vital role in MDS drying. Compared with conventional bio-drying and conventional thermal drying, the novel technique proposed in this study to assist microorganisms in drying MDS via PM addition and multisource thermal assistance has the advantages of high efficiency, time savings, and low cost. Thermal assistance not only promoted moisture evaporation but also shortened the activation time of the hyperthermophilic bacteria. The decomposition of organic matter by hyperthermophilic bacteria results in the production of a large amount of heat, which also promotes moisture evaporation. PM, which is livestock waste, was added to the MDS, effectively solving the problem of organic matter depletion caused by hyperthermophilic bacteria. In addition, the dried product can achieve heat recovery and utilization in subsequent thermal treatment, which is highly important for the large-scale treatment of MDS.

Process heat balance calculation

Under various optimization conditions, the heat balance calculation of the drying process in the MDS:PM = 4:1 system was investigated. The energy generation (input), consumption, and proportion of the system are shown in Fig. 7. Fig. 7a shows that the total energy generated (input) by the system was much greater than the energy consumption, indicating that the drying process was positive and spontaneous. In Fig. 7b, the proportion of Q_o was approximately 81.6 %, which proved that multisource heat recycling played a crucial role in system drying. However, the value of Q_o was lower than the accumulated energy consumption, indicating that single thermal drying cannot achieve rapid drying of the mixture, highlighting the importance of the synergistic effects of different processes to achieve rapid drying goals. In Fig. 7b, Q_{evapo} accounted for 86.43 %, which meant that most of the input heat energy was used for moisture reduction and that the system had a high utilization of energy (Yang et al., 2013). Previous studies have proposed the use of the drying efficiency η (η = Q_{evap}/Q_{bio}) to determine the energy acquisition mechanism of sludge drying. When η was in the range of 1.5–3.5, the microbial energy production capacity became an important energy source for the drying process under a low volatile solids content (Huilinir and Villegas, 2015; Navaee-Ardeh et al., 2010). In this study, η was 4.60, indicating again that the energy for sustaining system drying was synergistically obtained from biological and thermal drying. Multisource heat reuse also contributed significantly to the final drying effect. Q_{dryair} + Q_{watvap} accounted for 4.68 %, which was attributed mainly to the heating of the gas. In real applications, the dried input air came from a subsequent high-temperature heat treatment process, making the input air temperature much higher than the chamber temperature, so the combination of heat consumed by aeration would be further reduced. The energy consumed by increasing the substrate temperature (Q_{water} + Q_{solid}) and mechanical heat loss (Q_{radi} + Q_{condu} + $Q_{turning}$) was 5.17 % and 4.70 %, respectively, which was negligible. This heat loss was caused by multiple energy transfer mechanisms and could be reduced by improving the thermal insulation of the biodrying equipment. Therefore, according to the process of heat balance calculation, in practical applications, in addition to improving the utilization

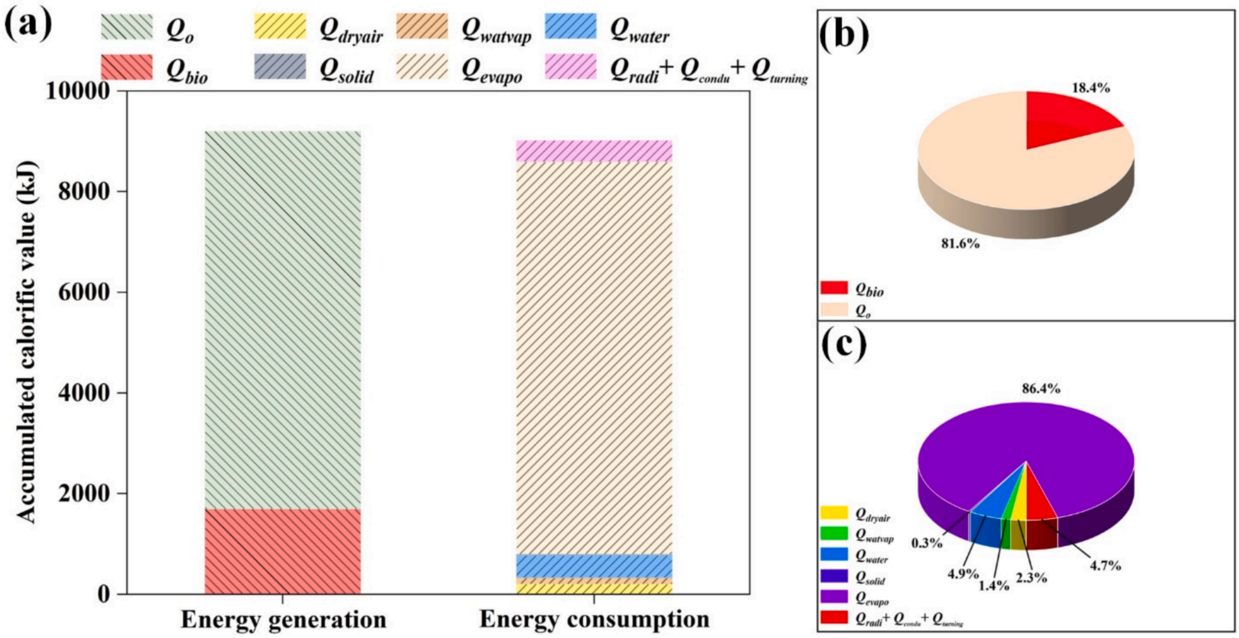

Fig. 7. (a) Energy generation (input) and energy consumption cumulative calorific value, (b) proportion of energy generation (input), and (c) proportion of energy consumption of the drying system.

efficiency of multisource heat reuse, equipment optimization is needed to reduce energy loss.

Cost analysis

The cost of the sludge drying system mainly included the cost of electricity, auxiliary materials, and labor handling. Electricity consumption was used mainly for equipment operation, which was reflected in the heating system, ventilation system, and turning system. The rated operating power of the equipment was approximately 0.29 kW, and the power consumption was 6.96 kWh for 24 h. According to the standard industrial electricity sales price in Jiangsu Province, China (the power supply voltage level was 220 kV:US $0.073/kWh (¥0.53/kWh)), the cost of single power consumption was US $0.51 (¥3.68), amounting to US $12.76/ton (¥92.54/ton) of mixture material with MDS:PM = 4:1, considering that the initial moisture content of MDS was approximately 85 %. The above electricity cost was calculated on the basis of an equipment loading capacity of 40 kg (80 % utilization rate). After accounting for this utilization rate, the adjusted cost of electricity consumption for the mixture was US $15.95/ton (¥115.68/ton). The cost of auxiliary materials was attributed to the use of pig manure and bacterial agents. On the basis of the average market sales price, dried pig manure was approximately US$82.75/ton (¥600/ton). The MDS:PM ratio was determined to be 4:1; in other words, 1 ton of MDS was added to 0.25 tons of pig manure. Therefore, treating 1-ton MDS costs US $20.69 (¥150) of pig manure. The bacterial agent was selected from the JiuBang organic fermenter, which costs approximately US $0.69/ton (¥5/ton). The total cost of auxiliary materials needs to be US$21.38 (¥155). The labor cost was used to pay for the workers who were responsible for the operation and maintenance inspection of the machine, which was approximately US$4.55(¥33)/(ton·person). The cost of exhaust gas treatment was approximately US $0.69/ton (¥5/ton) with reference to the results of relevant studies (Bian et al., 2020). In short, the cost of bio-drying sludge treatment was approximately US$42.57/ton (¥308.68/ton). The final dried products had a moisture content of 31.43 % and a weight reduction of 69.10 % after the drying reaction. This significant decrease in moisture content led to a substantial reduction in the volume of sludge, thereby greatly reducing the cost associated with sludge storage and land usage. Compared with the guide price of MDS drying treatment in the "List of Operating Service Charges Catalog of Jiangsu Province Implementing Government Pricing Management (Version 2023)" issued by the Jiangsu Development & Reform Commission, the technology employed in this study, which blends MDS with PM and utilizes multisource heat-assisted microbial rapid drying, could save approximately US$11.46–16.84/ton (¥83-122.10/ton) in the treatment of MDS. This significant cost savings underscores the engineering and economic benefits of this drying technology.

Conclusion

In this study, a novel technique using PM addition and multisource thermal assistance to assist hyperthermophilic bacteria in sludge drying is proposed and implemented. The mechanical factors were optimally selected via orthogonal experiments, and the addition ratio of PM was determined to be MDS:PM = 4:1. After 24 h of drying, the moisture content, organic matter content and $Q_{net,V,Mad}$ of the final dried products were 31.43 ± 0.91 %, 72.47 ± 1.89 % and 16.94 ± 0.35 MJ/kg, respectively, which indicated that the obtained dried products not only met the limitations of the corresponding standards but also satisfied the requirements of heat recovery and utilization in the subsequent thermal treatment. Compared with conventional bio-drying and conventional thermal drying, the drying technology used in this study has the advantages of high efficiency, time savings, and low cost. The process heat balance revealed that the drying process was spontaneous. Multisource heat assistance accounted for 81.6 % of the total generated (input) energy, and 86.43 % of the energy was used for moisture evaporation, indicating high energy utilization of the drying system. The novel drying technology saved approximately US$11.46–16.84/ton (¥83-122.10/ton) of MDS treatment, which indicated that the drying technology used in this study has objective socioeconomic value and could help reduce the cost of treating MDS in practical applications. Additionally, in this study, the experimental scale was in the transition stage from small- to medium-sized trials. In subsequent studies, novel drying technology will be applied to the large trial level of the project, and additional types of organic waste addition will also be investigated.

CRediT authorship contribution statement

Chencheng Wang: Writing – original draft, Formal analysis. **Zhigang He:** Supervision, Resources. **Muhammad Usman:** Writing – review & editing, Validation, Supervision. **Mohamed Gamal El-Din:** Writing – review & editing, Supervision. **Zhigang Liu:** Supervision, Resources. **Zhijun Luo:** Supervision, Conceptualization. **He Li:** Validation, Methodology. **Dandan Xiao:** Writing – original draft, Validation. **Qunchao Qian:** Writing – review & editing, Supervision, Formal analysis, Conceptualization. **Zhiren Wu:** Writing – review & editing, Funding acquisition, Conceptualization.

Declaration of competing interest

The authors declare that they have no known competing financial interests or personal relationships that could have appeared to influence the work reported in this paper.

Acknowledgments

This research was funded by the Qinghai Province Key R&D and Transformation Program (2022-SF-137).

Appendix A. Supplementary material

Supplementary data to this article can be found online at https://doi.org/10.1016/j.wmb.2025.100193.

References

Ahn, H.K., Richard, T.L., Choi, H.L., 2007. Mass and thermal balance during composting of a poultry manure - Wood shavings mixture at different aeration rates. Process Biochem. 42, 215–223.
Bian, B., Shen, Y., Hu, X., Tian, G., Zhang, L., 2020. Reduction of sludge by a biodrying process: Parameter optimization and mechanism. Chemosphere 248.
Bilgin, M., Tulun, Ş., 2015. Biodrying for municipal solid waste: Volume and weight reduction. Environ. Technol. 36, 1–23.
Bux, M., Baumann, R., Quadt, S., Pinnekamp, J., Muhlbauer, W., 2002. Volume reduction and biological stabilization of sludge in small sewage plants by solar drying. Drying Technol. 20, 829–837.
Cai, L., Chen, T.-B., Gao, D., Yu, J., 2016. Bacterial communities and their association with the biodrying of sewage sludge. Water Res. 90, 44–51.
Cao, B., Zhang, T., Zhang, W., Wang, D., 2021. Enhanced technology based for sewage sludge deep dewatering: A critical review. Water Research 189.
Chang, H., Zhao, Y., Xu, A., Damgaard, A., Christensen, T.H., 2023. Mini-review of inventory data for the dewatering and drying of sewage sludge. Waste Manag. Res.
Cheng, H., Li, Y., Hu, Y., Guo, G., Cong, M., Xiao, B., Li, Y.-Y., 2021. Bioenergy recovery from methanogenic codigestion of food waste and sewage sludge by a high-solid anaerobic membrane bioreactor (AnMBR): mass balance and energy potential. Bioresour. Technol. 326.
Cui, Y., Lv, Z., Wang, W., Zhang, K., Li, W., Zhao, X., Xu, Z., 2022. A real-time analysis system for filtrate state in plate-and-frame filter press process based on the machine vision. Measurement 202.
Dong, G.F., Yan, H.B., Tang, H., Fan, Y., Gao, L., Gao, Z.Y., 2023. In situ synthesis of TiNiTa coating by laser cladding with orthogonal test method. Intermetallics 159, 107934.
Gao, L., Cao, Y., Wang, L., Li, S., 2022. A review on sustainable reuse applications of Fenton sludge during wastewater treatment. Frontiers of Environmental Science & Engineering 16.
García, C., Hernandez, T., Costa, F., 1991. The influence of composting on the fertilizing value of an aerobic sewage sludge. Plant and Soil 136, 269–272.
Hao, S., Ren, S., Zhou, N., Chen, H., Usman, M., He, C., Shi, Q., Luo, G., Zhang, S., 2020. Molecular composition of hydrothermal liquefaction wastewater from sewage sludge and its transformation during anaerobic digestion. J. Hazard. Mater. 383, 121163.
Hao, Z., Yang, B., Jahng, D., 2018. Spent coffee ground as a new bulking agent for accelerated biodrying of dewatered sludge. Water Res. 138, 250–263.
Hoang, S.A., Bolan, N., Madhubashani, A.M.P., Vithanage, M., Perera, V., Wijesekara, H., Wang, H., Srivastava, P., Kirkham, M.B., Mickan, B.S., Rinklebe, J., Siddique, K.H.M., 2022. Treatment processes to eliminate potential environmental hazards and restore agronomic value of sewage sludge: A review. Environ. Pollut. 293.
Huilinir, C., Villegas, M., 2015. Simultaneous effect of initial moisture content and airflow rate on biodrying of sewage sludge. Water Res. 82, 118–128.
Idris, A., Khalid, K., Omar, W., 2004. Drying of silica sludge using microwave heating. Appl. Therm. Eng. 24, 905–918.
Jin, L., Zhang, G., Tian, H., 2014. Current state of sewage treatment in China. Water Res. 66, 85–98.
Li, J., Hao, X., Shen, Z., Wu, Y., van Loosdrecht, M.C.M., 2023. Low-temperature drying of waste activated sludge enhanced by agricultural biomass toward self-supporting incineration. Science of the Total Environment 888.
Li, Q., Lu, X., Guo, H., Yang, Z., Li, Y., Zhi, S., Zhang, K., 2018. Sewage sludge drying method combining pressurized electro-osmotic dewatering with subsequent biodrying. Bioresour. Technol. 263, 94–102.
Li, Q., Zhang, K., Yang, Z., Guo, H., Zheng, X., Zhang, Q., Xiong, J., Lu, X., 2022. Dynamic changes of microbial community and moisture ratio during biodrying of sludge after electrodewatering. J. Environ. Manage. 324, 116366.
Li, Q., Zhi, S., Yu, X., Li, Y., Guo, H., Yang, Z., Zhang, S., 2019. Biodegradation of volatile solids and water mass balance of biodrying sewage sludge after electrodewatering pretreatment. Waste Manag. 91, 9–19.
Li, Y., Liu, Y., Yu, X., Li, Q., Zhang, R., Zhang, S., 2020. Enhancement of sludge electrodewaterability during biological conditioning. RSC Adv. 10, 3153–3165.
Liang, Y., Wang, R., Sun, W., Sun, Y., 2023. Advances in Chemical Conditioning of Residual Activated Sludge in China. Water 15.
Liang, Y., Xu, D., Feng, P., Hao, B., Guo, Y., Wang, S., Klemes, J.J., 2021. Municipal sewage sludge incineration and its air pollution control. J. Clean. Prod. 295.
Lin, T., Liao, Y., Dai, T., Ma, X., 2023. Investigation on codisposal technology of sludge and municipal solid waste based on numerical simulation. Fuel 343, 127882.
Liu, H., Qiao, H., Liu, S., Wei, G., Zhao, H., Li, K., Weng, F., 2023. Energy, environment and economy assessment of sewage sludge incineration technologies in China. Energy 264.
Liu, J., Li, J., Xu, D., Sellamuthu, B., 2020. Improving aerobic sludge granulation in sequential batch reactor by natural drying: Effluent sludge recovery and feeding back into reactor. Chemosphere 242.
Luo, J., Lin, J., Ma, R., Chen, X., Sun, S., Zhang, P., Liu, X., 2020. Effect of different ash/organics and C/H/O ratios on characteristics and reaction mechanisms of sludge microwave pyrolysis to generate biofuels. Waste Manag. 117, 188–197.
Lv, H., Wang, F., Liu, D., Zhang, Y., Gu, Y., Yuan, D., Xing, S., Wu, X., Yang, J., Zhang, W., Scott, K., 2018. Effects of Piecewise Electric Field Operation on Sludge Dewatering: Phenomena and Mathematical Model. Ind. Eng. Chem. Res. 57, 12468–12477.
Mason, I.G., 2009. Predicting biodegradable volatile solids degradation profiles in the composting process. Waste Manag. 29, 559–569.
Mohammed, M., Ozbay, I., Karademir, A., Isleyen, M., 2017. Pretreatment and utilization of food waste as energy source by biodrying process, International Scientific Conference on Environmental and Climate Technologies (CONECT). Riga, LATVIA, pp. 100–107.
Moustafa, M.H., Ali, S.I., Metwaly, T.S., Al-Shazely, M., Samhan, F.A., 2022. Dewatering sludge from primary and secondary clarifiers in Jabal Asfar wastewater treatment plants - case study. Desalin. Water Treat. 261, 57–75.
Navaee-Ardeh, S., Bertrand, F., Stuart, P.R., 2010. Key variables analysis of a novel continuous biodrying process for drying mixed sludge. Bioresour. Technol. 101, 3379–3387.
Olivier, J., Vaxelaire, J., 2005. Municipal sludge dewatering by belt filter press: effect of operating parameters. J. Chem. Technol. Biotechnol. 80, 948–953.
Qu, J., Wang, H., Wang, K., Yu, G., Ke, B., Yu, H.-Q., Ren, H., Zheng, X., Li, J., Li, W.-W., Gao, S., Gong, H., 2019. Municipal Wastewater Treatment in China: Development History and Future Perspectives.
Renqingcairang, Liu, X., Liu, J., Fang, J., 2022. Frost-heave characteristics of saturated lean clay fillers by orthogonal test design considering the static surcharge. Case Studies in Construction Materials 17, e01526.
Ruiz-Gómez, N., Quispe, V., Ábrego, J., Atienza-Martínez, M., Murillo, M.B., Gea, G., 2017. Copyrolysis of sewage sludge and manure. Waste Manag. 59, 211–221.
Shi, Z., Campanaro, S., Usman, M., Treu, L., Basile, A., Angelidaki, I., Zhang, S., Luo, G., 2021a. Genome-centric metatranscriptomics analysis reveals the role of hydrochar in anaerobic digestion of waste activated sludge. Environ. Sci. Tech. 55, 8351–8361.
Shi, Z., Usman, M., He, J., Chen, H., Zhang, S., Luo, G., 2021b. Combined microbial transcript and metabolic analysis reveals the different roles of hydrochar and biochar in promoting anaerobic digestion of waste activated sludge. Water Res. 205, 117679.
Tan, P., Liu, X.-h., Cao, B.-w., Chen, W., Feng, J.-y., Xiang, Z.-l., 2023. Experimental study on heat transfer performance of high-power spray cooling system based on multifactor orthogonal test. Case Studies in Thermal Engineering 49.
Tang, Q., Xing, J., Sun, Z., Gan, M., Fan, X., Ji, Z., Huang, X., Yang, R., 2022. Enhancing the Dewaterability of Oily Cold Rolling Mill Sludge Using Quicklime as a Conditioning Agent. ACS Omega 7, 44278–44286.
Teng, F., Tan, G., Liu, T., Zhang, T., Liu, Y., Li, S., Lei, C., Peng, X., Yin, H., Meng, D., 2023. Inoculation with thermophiles enhanced the food waste biodrying and complicated interdomain ecological networks between bacterial and fungal communities. Environ. Res. 231.
Usman, M., Hao, S., Chen, H., Ren, S., Tsang, D.C., Sompong, O., Luo, G., Zhang, S., 2019. Molecular and microbial insights toward understanding the anaerobic digestion of the wastewater from hydrothermal liquefaction of sewage sludge facilitated by granular activated carbon (GAC). Environ. Int. 133, 105257.
Usman, M., Shi, Z., Ren, S., Ngo, H.H., Luo, G., Zhang, S., 2020. Hydrochar promoted anaerobic digestion of hydrothermal liquefaction wastewater: Focusing on the organic degradation and microbial community. Chem. Eng. J. 399, 125766.
Usman, M., Shi, Z., Cai, Y., Zhang, S., Luo, G., 2023. Microbial insights towards understanding the role of hydrochar in enhancing phenol degradation in anaerobic digestion. Environmental Pollution 330, 121779.
Wang, Y., Wang, F., Ji, M., 2013. Characteristics of Emitted Odor and Discharged Condensate Water of Sludge Thermal Drying Project in Shenzhen Nanshan Thermal

Power Plant, International Conference on Environmental Biotechnology and Materials Engineering (EBME 2013). Tianjin, PEOPLES R CHINA, pp. 127–132.
Wei, H., Gao, B., Ren, J., Li, A., Yang, H., 2018. Coagulation/flocculation in dewatering of sludge: A review. Water Res. 143, 608–631.
Wei, L., Zhu, F., Li, Q., Xue, C., Xia, X., Yu, H., Zhao, Q., Jiang, J., Bai, S., 2020. Development, current state and future trends of sludge management in China: Based on exploratory data and CO2-equivaient emissions analysis. Environ. Int. 144, 106093.
Wu, W., Zhou, Z., Chen, L., Chen, G., Zhang, Y., Jiang, L., Qiu, Z., He, K., Wu, Z., 2019. Conditioning for excess sludge and ozonized sludge by ferric salt and polyacrylamide: Orthogonal optimization, rheological characteristics and floc properties. Chem. Eng. J. 373, 1081–1090.
Wu, X., Zhang, J., Xu, E., Liu, Y., Cheng, Y., Addy, M., Zhou, W., Griffith, R., Chen, P., Ruan, R., 2016. Microbial hydrolysis and fermentation of rice straw for ethanol production. Fuel 180, 679–686.
Yan, A., Li, J., Liu, L., Ma, T., Liu, J., Ni, Y., 2018. Centrifugal dewatering of blended sludge from drinking water treatment plant and wastewater treatment plant. J. Mater. Cycles Waste Manage. 20, 421–430.
Yang, B., Zhang, L., Lee, Y., Jahng, D., 2013. Novel bioevaporation process for the zero-discharge treatment of highly concentrated organic wastewater. Water Res. 47, 5678–5689.
Yang, G., Zhang, G., Wang, H., 2015. Current state of sludge production, management, treatment and disposal in China. Water Res. 78, 60–73.
Yu, B., Chen, T., Wang, X., Yang, J., Zheng, G., Fu, L., Huang, X., Wang, Y., 2023a. Insights into the effect mechanism of back-mixing inoculation on sewage sludge biodrying process: Biodrying characteristics and microbial community succession. Sci. Total Environ. 857, 159460.
Yu, B., Chen, T., Zheng, G., Yang, J., Huang, X., Fu, L., Cai, L., 2022. Water-heat balance characteristics of the sewage sludge biodrying process in a full-scale biodrying plant with circulated air. Waste Manag. 141, 220–230.
Yu, S., Deng, S., Zhou, A., Wang, X., Tan, H., 2023b. Life cycle assessment of energy consumption and GHG emission for sewage sludge treatment and disposal: a review. Frontiers in Energy Research 11.
Zhang, D., Luo, W., Yuan, J., Li, G., 2018. Cobiodrying of sewage sludge and organic fraction of municipal solid waste: Role of mixing proportions. Waste Manag. 77, 333–340.
Zhang, S., Wang, F., Mei, Z., Lv, L., Chi, Y., 2021. Status and Development of Sludge Incineration in China. Waste Biomass Valoriz. 12, 3541–3574.
Zhao, L., Gu, W.-M., He, P.-J., Shao, L.-M., 2010. Effect of air-flow rate and turning frequency on biodrying of dewatered sludge. Water Res. 44, 6144–6152.
Zhou, W., Tuersun, N., Zhang, Y., Wang, Y., Cheng, C., Chen, X., 2021. Optimization and system energy balance analysis of anaerobic codigestion process of pretreated textile dyeing sludge and food waste. J. Environ. Chem. Eng. 9.